CSIRO PUBLISHING

Aust. J. Chem. **2015**, *68*, 99–105
http://dx.doi.org/10.1071/CH13679

Full Paper

Characterization and Acidic Properties of AlMCM-41 Prepared by Conventional and Post-Synthesis Alumination

Maria J. F. Costa,[A,E] *Thiago Chellappa,*[D] *Antonio S. Araujo,*[A] *Viviane M. Fonseca,*[B] *Valter J. Fernandes Jr,*[A] *Rubens M. Nascimento,*[D] *and José G. A. Pacheco*[C]

[A]Federal University of Rio Grande do Norte, Institute of Chemistry, 59078-970, Natal RN, Brazil.
[B]Federal University of Rio Grande do Norte, Department of Textile Engineering, 59060-300, Natal RN, Brazil.
[C]Federal University of Pernambuco, Department of Chemical Engineering, 50740-521, Recife PE, Brazil.
[D]Federal University of Rio Grande do Norte, Department of Mechanical Engineering, 59060-300, Natal RN, Brazil.
[E]Corresponding author. Email: mariadedeia@hotmail.com

The catalysts analysed in the current work are variations of MCM-41. The properties of these highly ordered mesoporous aluminosilicates were adjusted by an isomorphous substitution of Si by a trivalent cation, in this case Al^{3+}, generating catalysts of the AlMCM-41 type. The materials were synthesized with a silicon/aluminium ratio of 40, through two methods of impregnation of the metal: conventional and post-synthesis alumination. With the aim of determining the density of the acid sites of the Al_{40}MCM-41 prepared by post-synthesis and conventional alumination, studies of the adsorption of *n*-butylamine probe molecule were carried out. Further, the studied material was characterized by thermogravimetry measurements, providing the profile of decomposition of the samples, which allowed calculation of the densities of the acid sites. The model-free kinetic algorithms were applied in order to determinate conversion and apparent activation energy. Comparison of energy-dispersive X-ray fluorescence and X-ray photoelectron spectroscopy measurements indicated that the post-synthesis method was more favourable based on the metal positioning, 'anchored' in the surface of the catalyst. The textural properties of the calcined Al_{40}MCM-41 prepared by post-synthesis and conventional alumination were characterized by X-ray diffraction, N_2 isothermal adsorption measurements (Brunauer–Emmett–Teller and Barrett–Joyner–Halenda), transmission electron microscopy, and X-ray photoelectron spectroscopy.

Manuscript received: 13 December 2013.
Manuscript accepted: 30 March 2014.
Published online: 23 June 2014.

Introduction

MCM-41 or Mobil composition of matter no. 41 (hexagonally ordered mesoporous silica), the main representative of a family of mesoporous materials denominated M-41S, was developed by a group of scientists of Mobil Oil Corporation. The most interesting feature of MCM-41 is its regular pore system, which consists of a hexagonal array of one-dimensional-shaped pores and pore diameter that can vary systematically from 2 to 10 nm.[1]

A high surface area and the capacity for generating surface acidity also are important characteristics of this material and it has attracted a great deal of attention, due to its potential applications in catalysis and adsorption technologies.[2–4] A previous study found that Al-containing MCM-41 catalysts are more catalytically active than microporous zeolite Y (zeolite Y exhibits the FAU (faujasite) structure, has a Si/Al ratio of 2.43 and Fd3m symmetry) for cumene cracking (as a medium to strong Brønsted acid-catalyzed model reaction) and 2-propanol dehydration reactions (as a weak Lewis and Brønsted acid-catalyzed model reaction).[4]

The starting point to be considered, in the current work, was the preparation of materials substituting Al heteroatoms for Si; this could be adjusted by the isomorphous substitution of Si by a trivalent cation (Al^{3+}), thus producing the AlMCM-41 mesoporous material.[5,6] The incorporation of aluminium into the MCM-41 structure was accomplished through two distinct methods, denoted as the conventional and post-synthesis (PS) methods, with the intention of obtaining the best conditions for the production of Al_{40}MCM-41, where 40 is the silicon/aluminium ratio.

In the scientific literature, there are studies that mention that the pore diameter and the thermal stability of samples of Al-MCM-41 decrease gently with increasing Al content. However, PS-modified Al-MCM-41 possesses better thermal stability, and this method also permits the incorporation of more aluminium without destroying the mesoporous structure compared with Al-MCM-41 prepared by the conventional method.[7]

In this study, the acid properties were studied using adsorption of *n*-butylamine probe molecule; further, the

thermodesorption was studied using thermogravimetric analysis (TGA) measurements. Also, some kinetic parameters were determined, employing integral TG curves, as well as a model-free kinetics method.[8–10]

Currently, thermal analysis is applied in a large variety of scientific applications. It provides efficient tools for measuring thermodynamic properties such as enthalpies, heat capacities, and the temperature of phase transitions.[11] Through TGA, it is possible to follow the kinetics of thermally stimulated processes, such as volatilization, decomposition, oxidation, reduction, crystallization, polymerization, and combustion.

Isoconversional methods, such as those performed in the current work, require experiments with different heating rates, in order to ensure the appropriate calculation of the activation energy as a function of conversion. The potential applications of the isoconversional methods have been studied by Vyazovkin, showing that it can be used to explore reaction mechanisms and predict process kinetics. These two features allow a foundation of isoconversional kinetic analysis, so-called 'model-free kinetics'.[12]

The model-free kinetics method proposed by Vyazovkin[13–17] has been previously applied to determine kinetic parameters of some chemical reactions, such as apparent activation energies (E_a) and conversion rates.

Experimental

The Al_{40}MCM-41 sample prepared by conventional alumination was synthesized through the hydrothermal method, based on an adapted experimental procedure,[18,19] thus possessing a similar MCM-41pattern, with a molar composition of $4.58SiO_2 : 0.494Na_2O : 0.057Al_2O_3 : 1CTMABr : 200H_2O$ (CTMABr, cetyltrimethylammonium bromide).

Aqueous solutions of silica gel (Merck, 95 % SiO_2) were used as the silicon source, alongside sodium silicate (Riedel-de Haën, 60 % SiO_2 and 18 % Na_2O) as a sodium source, and these were further combined with a solution of pseudoboehmite (Vista, 70 % Al_2O_3) as an aluminium source. Cetyltrimethylammonium bromide (Vetec, 98 % CTMABr) was used as a template structure. Typically, the synthesis procedure to obtain 1.3 g of dry-basis material was: (i) 0.861 g of silica, 0.787 g of sodium silicate, and 8.362 g of distilled water were stirred at 60°C for 2 h, producing a white gelatinous suspension; (ii) 0.026 g of pseudoboehmite was placed in 2.0 mL of distilled water and stirred at 60°C for 30 min. Solution (ii) was added to solution (i) and stirred at 60°C for 30 min. A solution (iii) prepared from 1.751 g of CTMABr and 6.362 g of distilled water was added to the (i) + (ii) mixture and stirred for 1 h at room temperature. Following the preparation of the hydrogel, it was transferred to a Teflon-lined stainless steel autoclave, where the process of crystallization of the material was performed at 100°C with a pH of 9–10 for 4 days. For pH adjustment, 50 % acetic acid in distilled water was used. The obtained material was filtered, washed with water, and dried at 100°C in a stove for 2 h with the intention of obtaining the sodium form Na-Al_{40}MCM-41 prepared by conventional alumination. Afterwards, the mesoporous material underwent a calcination step to remove the template from the catalyst pores at 450°C for 1 h in an N_2 atmosphere and then for 1 h in synthetic air atmosphere (mixture of N_2 and O_2) at the same temperature using a dynamic flow of 100 mL min^{-1}. The temperature was increased from room temperature to 450°C at a heating rate of 10°C min^{-1}.

The Al_{40}MCM-41(PS) sample prepared by post-synthesis alumination was also synthesized through the hydrothermal method, in the same way as described previously, but without the addition of the aluminium source to the synthesis mixture, and with a molar composition $4.58SiO_2 : 0.494Na_2O : 1CTMABr : 200H_2O$. The impregnation of aluminium on the MCM-41 mesoporous material, generating Al_{40}MCM-41(PS), occurred from the contact of ~1 g of MCM-41 synthesized and calcined with 1 mL of aqueous ammonia (Vetec, NH_4OH, 28–30 %) and 5 mL of a 0.0815 M aqueous solution of aluminium nitrate nonahydrate (Vetec, $Al(NO_3)_3{\cdot}9H_2O$).

The corrected mass for the calcined MCM-41 and the relative concentration for the solution of the aluminium source were calculated based on a silicon/aluminium ratio of 40. The final mixture was stirred at 60°C for 1 h, using a reflow process to minimize evaporation. The gel was filtered, washed with water, and dried at 100°C in a stove for 2 h to obtain the sodium form Na-Al_{40}MCM-41(PS). Afterwards, the mesoporous material underwent a thermal treatment step to decompose the precursor salt of aluminium to its corresponding oxide on the surface support at 450°C for 2 h in synthetic air using a dynamic flow of 100 mL min^{-1}. The temperature was increased from room temperature to 450°C at a heating rate of 10°C min^{-1}. The methodology used to impregnate aluminium on mesoporous MCM-41 was based on thermogravimetric analysis, which revealed that the decomposition of aluminium nitrate in an air atmosphere occurs at temperatures below 450°C.

Acid forms of the Al_{40}MCM-41 materials prepared by conventional and PS alumination were obtained by heating ~0.5 g of each material under reflux twice with 250 mL of a 0.650 M aqueous solution of ammonium chloride (Vetec, NH_4Cl) for 2 h at 60°C, followed by a thermal treatment step at 450°C for 1 h in synthetic air.

In order to evaluate and analyse the strength and type of acid sites, *n*-butylamine adsorption on the HAl_{40}MCM-41 samples was carried out in a reactor containing ~0.1 g of catalyst, which was initially activated at 400°C under nitrogen flow for 2 h. After this activation, the temperature was reduced to 95°C and the nitrogen flow was passed through in a bubbler flask containing liquid *n*-butylamine. The *n*-butylamine-saturated nitrogen stream was passed through the reactor containing the samples for 40 min. Afterwards, pure nitrogen was passed, once more, over the samples for another 40 min, in order to remove the physically adsorbed *n*-butylamine. Also, thermodesorption of the *n*-butylamine probe molecule was performed using TG measurements. TG analyses were carried out on Mettler equipment (model TGA/SDTA851) using nitrogen as carrier gas flowing at 25 mL min^{-1}. Samples of ~10 mg were heated in alumina crucibles from room temperature up to 900°C at heating rates of 5, 10, and 20°C min^{-1}.

The model-free kinetics proposed by Vyazovkin et al.[12–17] were used to evaluate the kinetic parameters of the degree of thermodesorption of the probe molecule from the HAl_{40}MCM-41 samples, such as apparent activation energy, conversion rates, and thermodesorption time of the probe molecule as a function of temperature.

The calculations were performed using the Mettler–Toledo *STARe* software; thus, the best conditions for alumination of the mesoporous system of AlMCM-41 were determined.

X-ray diffraction (XRD) measurements were carried out using CuK_α radiation with a 2θ angle range of 1–7° for calcined samples, with a step of 0.02°, on Shimadzu XRD 6000 X-ray equipment. Surface area, pore volume, and pore distribution were obtained through Brunauer–Emmett–Teller (BET)[20] and

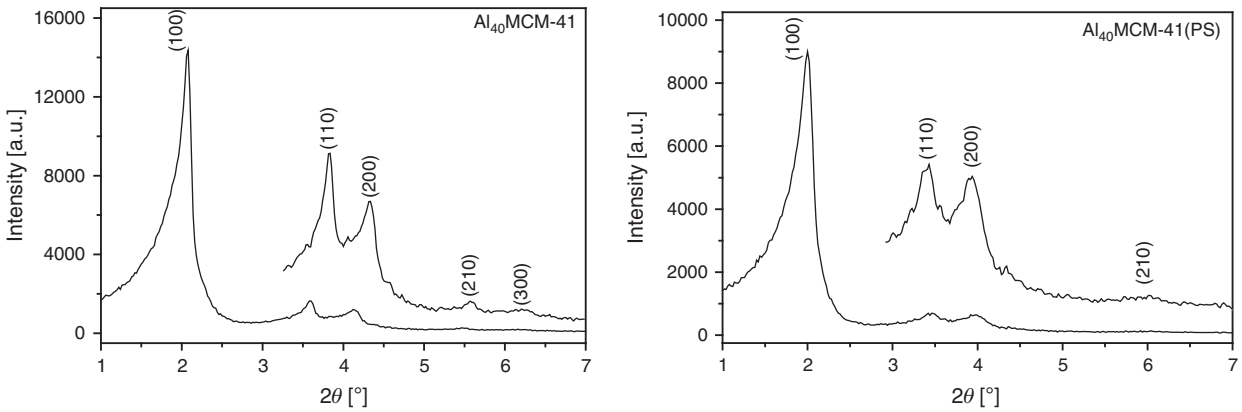

Fig. 1. Low-angle X-ray diffraction spectra of calcined samples. PS: post-synthesis.

Barrett–Joyner–Halenda (BJH) [21] methods using nitrogen adsorption isotherms at 77 K (Quantachrome instrument, Anova-2000 model). Transmission electron microscopy (TEM) measurements and energy-dispersive X-ray fluorescence (EDX) spectra were obtained using a Philips CM200 instrument with an electron beam accelerating voltage of 200 kV; the samples were dispersed ultrasonically in H_2O at a concentration of 1 mg mL^{-1}, and a drop of the suspension was deposited on a carbon copper grid, and then dried.[22]

Surface studies through X-ray photoelectron spectroscopy (XPS) were carried out with a Physical Electronics PHI-750 spectrometer, equipped with an MgK_α (1253.6 eV) X-ray radiation source. In order to measure binding energies (±0.1 eV), the C 1s signal of adventitious carbon was used as reference at 284.8 eV. All samples were degassed for 12 h under ultra-high vacuum ($<1.3 \times 10^{-6}$ Pa) before the analysis. The modified Auger parameter of Al (α') was calculated using the following Eqn 1.[23]

$$\alpha' = \mathrm{KE(Al(KLL))} + \mathrm{BE(Al\ 2p)} \quad (1)$$

where KE(Al(KLL)) is the kinetic energy of the Auger electron of Al($KL_{23}L_{23}$) and BE(Al 2p) is the binding energy of the Al 2p XPS peak.

Results and Discussion

Physicochemical Characterization

The spectra obtained from low-angle X-ray diffraction of the calcined Al_{40}MCM-41 samples prepared by conventional and PS alumination is presented in Fig. 1a and b respectively.

Characteristic diffraction peaks were seen for these materials, namely (100), (110), (200), (210), and (300),[1] and it was possible to obtain the hexagonal structure parameter a_0 from the main interplanar distance ($d_{(100)}$). The value a_0 represents the sum of the pore diameter (D_p) and the silica wall thickness (W_t). Eqn 2 correlates the interplanar distances with the value of the hexagonal structure parameter.[22] Using reflection (100), a simplified expression is derived from Eqn 3 that correlates the $d_{(100)}$ value with a_0. Eqn 4 is used to obtain the value of the median wall thickness (W_t), combining the XRD with BJH data.[24] The a_0 values obtained through (100) XRD reflection of Al_{40}MCM-41 samples prepared by conventional and PS alumination were 4.90 and 4.35 nm respectively.

$$\frac{1}{d(hkl)^2} = \frac{4(h^2 + hk + l^2)}{3a_0^2} + \frac{l^2}{c} \quad (2)$$

$$a_0 = \frac{2d_{(100)}}{\sqrt{3}} \quad (3)$$

$$W_t = a_0 - D_p \quad (4)$$

where h, k, l are the Miller indices and c is a lattice parameter for hexagonal crystal structure.

The nitrogen adsorption–desorption phenomenon provides a technique to determine surface area, pore volume, and pore size distribution. The surface area has been obtained by correlating the relative pressure (P/P_0) data in the range of 0.05–0.3 by the BET method[20]. The N_2 adsorption–desorption isotherms for the calcined Al_{40}MCM-41 samples prepared by conventional and PS alumination are shown in Fig. 2a.

It can be seen that the samples exhibit a type IV nitrogen adsorption–desorption isotherm, typical of a uniform mesoporous material, according to IUPAC nomenclature.[25] The isotherms exhibit three stages as follows: adsorption at low pressure ($P/P_0 < 0.28$) accounts for a monolayer adsorption of nitrogen on the walls of the mesopores. As the relative pressure increases, the isotherms rise steeply (at $P/P_0 \sim 0.28$), which is characteristic of capillary condensation within mesopores, having a narrow hysteresis loop. At higher relative pressures ($P/P_0 > 0.4$), the plateau region is due to multilayer adsorption on the outer surface of the particles. The total surface area of the synthesized conventional Al_{40}MCM-41, calculated according to the BET method, was 795 m^2 g^{-1} and for Al_{40}MCM-41(PS) was 794 m^2 g^{-1}.

The pore size distribution determined from the adsorption isotherm by the BJH method[21] covered a pore diameter range of 2–20 nm. As shown in Fig. 2b, a very narrow distribution was obtained for the Al_{40}MCM-41 material prepared by conventional and PS alumination, with a median pore diameter of 4.1 and 3.2 nm and a mesopore volume of 0.94 and 0.27 cm^3 g^{-1} respectively. The channel wall thickness calculated by applying Eqn 3, based on XRD and BJH data, was 0.8 and 1 nm respectively.

Fig. 3a, b shows, respectively, TEM images of the calcined Al_{40}MCM-41 samples that were prepared by conventional and PS alumination. It can be seen that the mesopores possess a highly ordered hexagonal array arrangement that is apparently

long-range. On one hand, this observation corroborates the XRD low-angle pattern, where all diffraction peaks were seen and not only the main (100) reflexion (as observed for Al_{40}MCM-41, which is disordered). On the other hand, the uniform porosity channels revealed by TEM images are in agreement with the quite narrow pore-size distribution determined by N_2 adsorption (BJH).

Table 1 shows the results of the Al_2O_3 and SiO_2 content analysis and surface Si/Al atomic ratio determined by EDX measurement of calcined Al_{40}MCM-41 samples prepared by

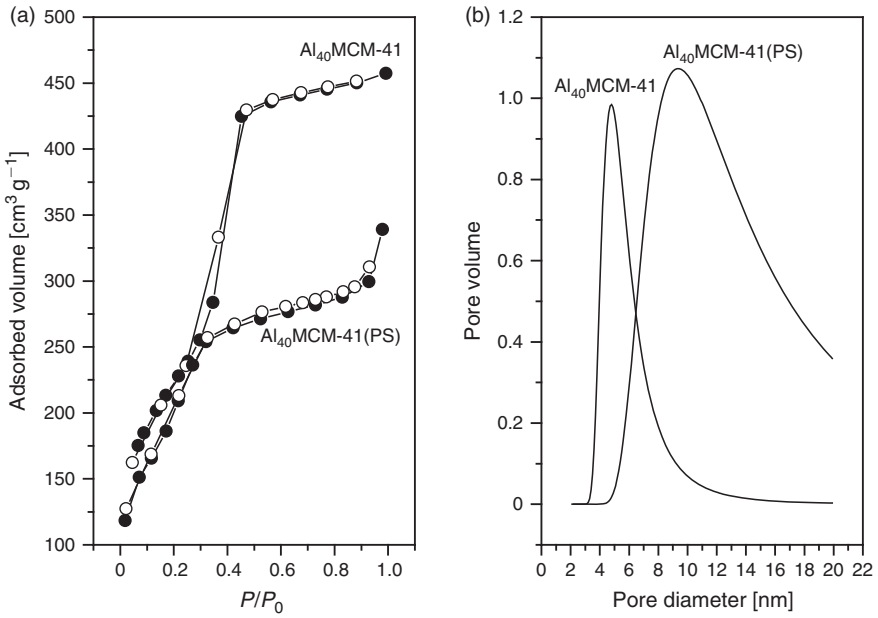

Fig. 2. Nitrogen adsorption isotherms and pore distributions of the Al_{40}MCM-41 material prepared by conventional and post-synthesis (PS) alumination: (a) adsorption–desorption isotherms, and (b) pore size distribution (nm).

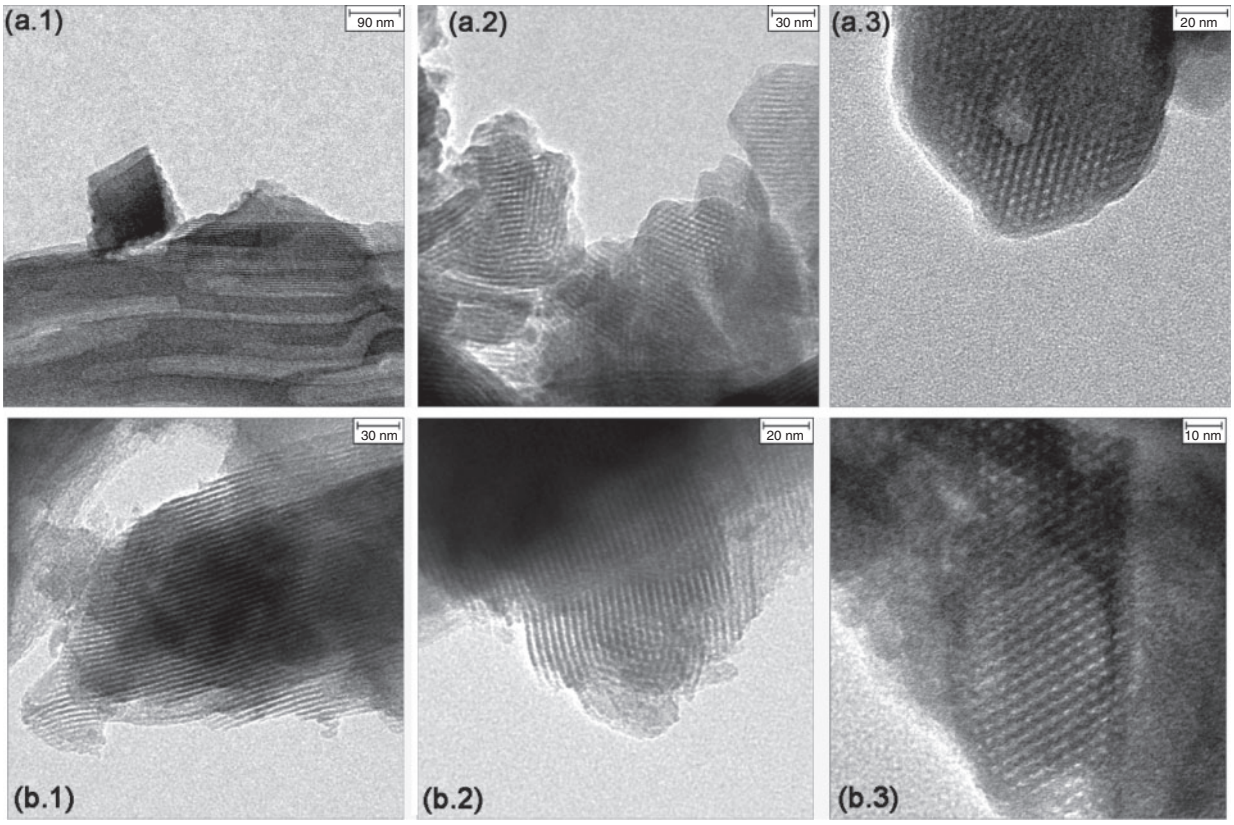

Fig. 3. Transmission electron microscopy image showing highly ordered, long-range hexagonal array of mesopores in Al_{40}MCM-41 samples prepared by (a.1, a.2 and a.3) conventional, and (b.1, b.2 and b.3) post-synthesis alumination.

conventional and PS alumination. Results show that the PS-modified material possesses a surface Si/Al atomic ratio of 11.1, lower than in the conventional material, which has a ratio of 23.3, and indicates the PS method is more favourable based on the metal positioning, as the metal is 'anchored' in the surface of the catalyst. The PS method also allows the incorporation of more aluminium without disintegration of the mesoporous structure compared with Al-MCM-41 prepared by conventional hydrothermal synthesis.

In order to gain insight into the surface composition, XPS was employed in the current study. Table 2 shows the BE and atomic concentration of Al 2p, Si 2p, C 1s and O 1s, surface Si/Al atomic ratio determined by XPS for the calcined materials and the calculated modified Auger parameter of Al (α').

Results showed that the PS-modified material possesses a surface Si/Al atomic ratio of 16.4, lower than in the conventional material, with 28.4, confirming the theory that it is possible to incorporate more aluminium without disintegration of the mesoporous structure when compared with Al-MCM-41 prepared by conventional hydrothermal synthesis. This result was as expected, because aluminium has been incorporated by PS and consequently, aluminium atoms would be preferentially located on the inner surface of the pores. The BE of the Al 2p peak appears at 74.6 and 74.7 eV for Al_{40}MCM-41 material prepared by conventional and PS alumination respectively.

The Auger parameter of Al (α') was 1461.5 and 1461.6 eV for Al_{40}MCM-41 material prepared by conventional and PS alumination respectively. The use of α' allows a clear distinction between tetrahedral and octahedral Al. For well-known aluminosilicates, the α' values fall between 1461.3 and 1461.6 eV for octahedral aluminium, and between 1460.3 and 1460.6 eV for tetrahedral aluminium. Therefore, when our data was compared with the scientific literature, both samples clearly showed that they are characteristic of octahedral aluminium.[23,26]

Total Surface Acidity Measurement by n*-Butylamine Probe Molecule Thermodesorption*

Fig. 4 shows the TGA/DTG (derivative thermogravimetric analysis) curves used for the calculation of the acid site concentration for the samples synthesized by different methods.

The different profiles observed in Fig. 4 are evidence of the influence of the preparation method on the samples. The sample synthesized by the conventional method showed essentially one step attributed to the thermodesorption of physically adsorbed *n*-butylamine, whereas the sample prepared using the PS method clearly showed two steps.

The chemical desorption of *n*-butylamine from acid sites occurred in the temperature range of 100–550°C (strong acid sites, T = 100–300°C; moderate acid sites, T = 300–550°C) and the peaks were used for calculation of acid sites concentration. The total density of acid sites was 0.99 and 1.43 mmol g^{-1} for the conventional and PS method respectively. The higher acidity of PS-alumination catalyst may be attributed to the location of the aluminium preferentially on the surface. The catalyst prepared by the conventional method may have more aluminium in the crystal lattice. It was also observed that the aluminium content in the PS catalyst was twice as high as in the conventional catalyst, providing more active sites from the aluminium oxide (see Table 1).

The activation energies for thermodesorption of *n*-butylamine for both samples were calculated using dynamic integral TG curves at three heating rates and the results are shown in Fig. 5.

The values of activation energy obtained using model-free kinetics (Fig. 5) had different profiles. The sample produced using the PS method showed values for E_a of 78.2 ± 4.2 kJ mol^{-1} whereas the sample prepared using the conventional method showed a higher variation in the values. The conventional catalyst had an activation energy varying from 80 to 135 kJ mol^{-1} in the thermodesorption conversion range of 60–100 %. This fact could indicate that the distribution of the metal in the material surface when obtained with the PS method is increased. That behaviour was also shown from the conversion graph (Fig. 4b). The percentage degradation or conversion as a function of time for different temperatures was calculated (Fig. 4b) and it could be seen that in the sample obtained by the conventional method, conversion time decreased considerably as a function of temperature when compared with that from the PS method.

The study to determine adsorption of the *n*-butylamine probe molecule is an important variable in the determination of the final properties of the Al_{40}MCM-41 materials prepared by PS and conventional alumination, and these results are useful for ascertaining the density of the acid sites. Vyazovkin[12–17] developed an integral method of model-free kinetic analysis that has multiple heating rates and allows an evaluation of both simple and complex kinetics reactions. The rate of the chemical reactions depends on the conversion (α), temperature (T), and time (t). The analysis is based on the isoconversion principle, which states that the constant conversion of the reaction rate is only a function of temperature. In a typical experiment, it is necessary to obtain at least three different heating rates (β) and the respective conversion curves are evaluated from the measured TG curves. For each conversion (α), $\ln(\beta/T_\alpha^2)$ plotted vs

Table 1. Results of energy-dispersive X-ray fluorescence (EDX) measurements for the Al_{40}MCM-41 samples prepared by conventional and post-synthesis (PS) alumination

Sample	Al_2O_3 [%]	SiO_2 [%]	Si/Al atomic ratio
Al_{40}MCM-41	2.1	97.8	23.3
Al_{40}MCM-41(PS)	4.3	95.7	11.1

Table 2. Binding energy, atomic concentration, Si/Al atomic ratio, and Auger parameter of Al (α') determined by X-ray photoelectron spectroscopy for the calcined materials

Sample	Binding energy [eV]				Atomic concentration				Si/Al atomic ratio	Auger parameter of Al (α') [eV][A]
	C 1s	O 1s	Al 2p	Si 2p	C 1s	O 1s	Al 2p	Si 2p		
Al_{40}MCM-41	284.8	532.2	74.6	103.0	5.1	64.0	1.0	29.8	28.4	1461.5
Al_{40}MCM-41(PS)	284.9	532.7	74.7	103.1	7.2	61.9	1.8	29.0	16.4	1461.6

[A]Data taken from van den Brand et al.[26] KE(Al(KLL)) of the alkaline pretreated = 1386.9 eV.

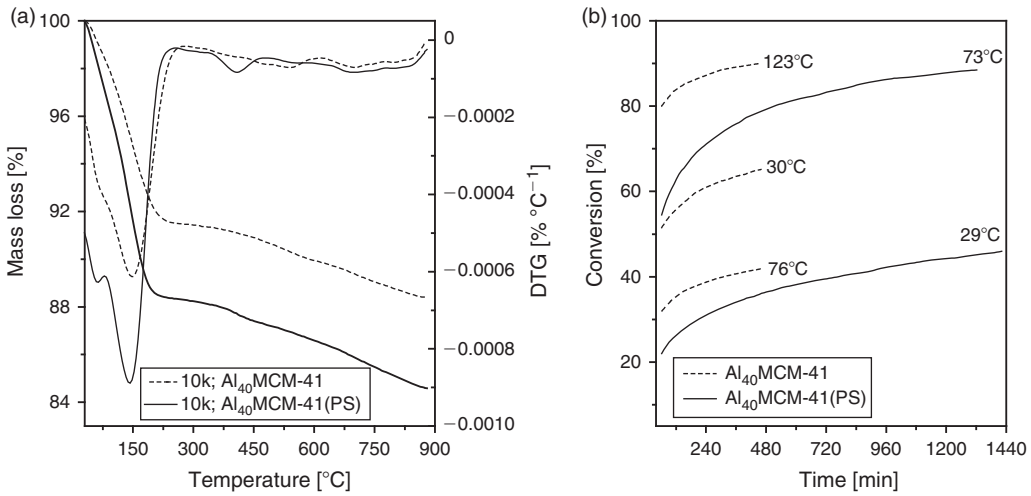

Fig. 4. (a) Thermogravimetric analysis/derivative thermogravimetric analysis curves, and (b) thermodesorption conversion of *n*-butylamine as a function of time at different temperatures for the Al_{40}MCM-41 catalysts prepared by conventional and post-synthesis (PS) alumination (10k = heating rate of 10°C min^{-1}).

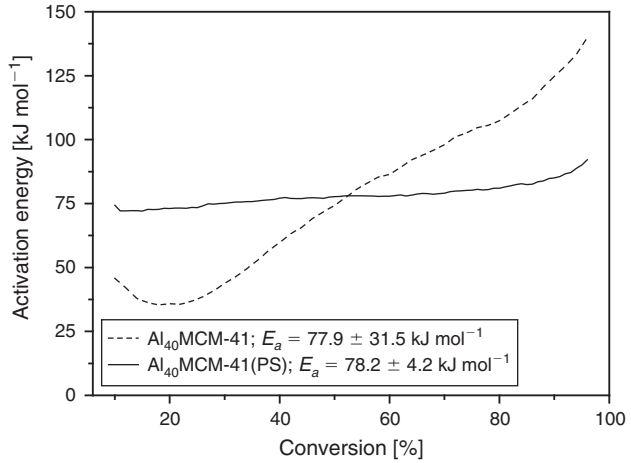

Fig. 5. Apparent activation energy for thermodesorption of the *n*-butylamine probe molecule on Al_{40}MCM-41 samples prepared by conventional and post-synthesis (PS) alumination.

$1/T_\alpha$ gives a straight line with slope $-E_a/R$ (Eqn 5), and therefore the activation energy is obtained as a function of conversion.

$$\ln\left(\frac{\beta}{T_\alpha^2}\right) = \ln\left[\frac{R \cdot k_0}{E_a \cdot g(\alpha)}\right] - \frac{E_a}{R} \cdot \frac{1}{T_\alpha} \qquad (5)$$

Conclusions

A successful synthesis of pure and highly ordered AlMCM-41 was obtained via a hydrothermal process. The textural properties of the nanostructured material obtained were evaluated by means of XRD and nitrogen adsorption analyses; the values of mean pore diameter (*Dp*) and hexagonal structure parameter (a_0) were obtained. Based on these parameters, silica wall thicknesses (W_t) were calculated to be 0.8 and 1 nm for Al_{40}MCM-41 samples prepared by conventional and PS alumination. TEM observations confirmed that the Al_{40}MCM-41 synthesized by conventional and PS methods possesses a highly ordered, long-range hexagonal array of mesopores. XPS and *n*-butylamine adsorption studies confirmed that the PS method is a good route for incorporating aluminium into mesoporous silica MCM-41.

Acknowledgements

This study was supported by the National Council of Technological and Scientific Development of Brazil (CNPq). Also, one of the authors (MJFC) acknowledges CNPq for the auxiliary research funding and fellowship.

References

[1] M. Oliverio, A. Procopio, T. N. Glasnov, W. Goessler, C. O. Kappe, *Aust. J. Chem.* **2011**, *64*, 1522. doi:10.1071/CH11125
[2] R. Franchi, P. J. E. Harlick, A. Sayari, *Stud. Surf. Sci. Catal.* **2005**, *156*, 879. doi:10.1016/S0167-2991(05)80300-3
[3] N. Hondow, J. Harowfield, G. Koutsantonis, G. Nealon, M. Saunders, *Microporous Mesoporous Mater.* **2012**, *151*, 264. doi:10.1016/J.MICROMESO.2011.10.027
[4] S. K. Jana, H. Takahashi, M. Nakamura, M. Kaneko, R. Nishida, H. Shimizu, T. Kugita, S. Namba, *Appl. Catal. A Gen.* **2003**, *245*, 33. doi:10.1016/S0926-860X(02)00616-6
[5] S. Ajaikumar, A. Pandurangan, *J. Mol. Catal. Chem.* **2007**, *266*, 1. doi:10.1016/J.MOLCATA.2006.10.010
[6] N. Saadatjoo, M. Golshekan, S. Shariati, H. Kefayati, P. Azizi, *J. Mol. Catal. Chem.* **2013**, *377*, 173. doi:10.1016/J.MOLCATA.2013.05.007
[7] L. Y. Chen, Z. Ping, G. K. Chuah, S. Jaenicke, G. Simon, *Microporous Mesoporous Mater.* **1999**, *27*, 231. doi:10.1016/S1387-1811(98)00257-1
[8] A. S. Araujo, V. J. Fernandes, Jr, M. J. B. Souza, O. S. A. Silva, J. M. F. B. Aquino, *Thermochim. Acta* **2004**, *413*, 235. doi:10.1016/J.TCA.2003.10.002
[9] H. Polli, L. A. M. Pontes, A. S. Araujo, J. M. F. Barros, V. J. Fernandes, Jr, *J. Therm. Anal. Calorim.* **2009**, *95*, 131. doi:10.1007/S10973-006-7781-1
[10] S. Arias, M. M. Prieto, B. Ramajo, A. Espina, J. R. García, *J. Therm. Anal. Calorim.* **2009**, *98*, 457. doi:10.1007/S10973-009-0301-3
[11] R. P. Rodríguez, R. Sierens, S. Verhelst, *J. Therm. Anal. Calorim.* **2009**, *96*, 897. doi:10.1007/S10973-009-0043-2
[12] S. Vyazovkin, N. Sbirrazzuoli, *Macromol. Rapid Commun.* **2006**, *27*, 1515. doi:10.1002/MARC.200600404
[13] S. Vyazovkin, V. Goryachko, *Thermochim. Acta* **1992**, *194*, 221. doi:10.1016/0040-6031(92)80020-W
[14] S. Vyazovkin, *Int. J. Chem. Kinet.* **1996**, *28*, 95. doi:10.1002/(SICI)1097-4601(1996)28:2<95::AID-KIN4>3.0.CO;2-G

[15] S. Vyazovkin, N. Sbirrazzuoli, *Anal. Chim. Acta* **1997**, *355*, 175. doi:10.1016/S0003-2670(97)00505-9
[16] S. Vyazovkin, C. A. Wight, *Int. Rev. Phys. Chem.* **1998**, *17*, 407. doi:10.1080/014423598230108
[17] S. Vyazovkin, C. A. Wight, *Thermochim. Acta* **1999**, *53*, 340.
[18] M. J. B. Souza, A. O. S. Silva, V. J. Fernandes, Jr, A. S. Araujo, *J. Therm. Anal. Calorim.* **2005**, *79*, 425. doi:10.1007/S10973-005-0078-Y
[19] F. W. T. Goh, Z. Liu, X. Ge, Y. Zong, G. Du, T. S. A. Hor, *Electrochim. Acta* **2013**, *114*, 598. doi:10.1016/J.ELECTACTA.2013.10.116
[20] S. Brunauer, P. H. Emmett, E. Teller, *J. Am. Chem. Soc.* **1938**, *60*, 309. doi:10.1021/JA01269A023
[21] E. P. Barrett, L. G. Joyner, P. P. Halenda, *J. Am. Chem. Soc.* **1951**, *73*, 373. doi:10.1021/JA01145A126
[22] M. J. B. Souza, A. S. Araujo, A. M. G. Pedrosa, B. A. Marinkovic, P. M. Jardim, E. Morgado, Jr, *Mater. Lett.* **2006**, *60*, 2682. doi:10.1016/J.MATLET.2006.01.066
[23] M. J. Remy, M. J. Genet, G. Poncelet, P. F. Lardinois, P. P. Notte, *J. Phys. Chem.* **1992**, *96*, 2614. doi:10.1021/J100185A041
[24] M. Kruk, M. Jaroniec, Y. Sakamoto, O. Terasaki, R. Ryoo, H. Ko, *J. Phys. Chem. B* **2000**, *104*, 292. doi:10.1021/JP992718A
[25] K. S. W. Sing, D. H. Everett, R. A. W. Haul, L. Moscow, R. Apierotti, T. Rouquerol, T. Siemienewska, *Pure Appl. Chem.* **1985**, *57*, 603. doi:10.1351/PAC198557040603
[26] J. van den Brand, P. C. Snijders, W. G. Sloof, H. Terryn, J. H. W. de Wit, *J. Phys. Chem. B* **2004**, *108*, 6017. doi:10.1021/JP037877F